# AUTOMATIC DETERMINATION OF THE MAGNETIZATION-TO-DENSITY RATIO AND THE MAGNETIZATION INCLINATION BASED ON THE POISSON THEOREM (2D SOURCES)

Carlos A Mendonça, Depto. de Geofísica, IAG/USP



**Abstract**

The Poisson theorem establishes a linear relationship between the gravity and magnetic potentials arising from common dense and magnetized bodies. This article presents analytical solutions derived from the Poisson's theorem that allow to determine the magnetization-to-density-ratio and the magnetization direction of the sources. Because the obtained solutions relate 2D gravity and magnetic vector fields, a processing scheme is proposed in order to obtain the related vector fields from the measured field components. Results from tests with synthetic data are discussed.

**Introduction**

The Poisson theorem (Garland, 1951; Grant and West, 1965; Cordell and Taylor, 1971; Chandler et al., 1981) establishes a linear relationship between the gravity and magnetic potentials and, by extension, the corresponding anomalies. For the joint interpretation of potential field data, the Poisson theorem has been used to determine the MDR - magnetization-to-density ratio (Garland, 1951; Kanasewich and Argawal, 1970; Bott and Ingles, 1972; Chandler et al., 1981; Hildebrand, 1985; Chandler and Malek, 1991) and, less often, the magnetization direction of single dense and magnetic structures (Ross and Lavin, 1966; Cordell and Taylor, 1971). None of the existing methods, however, is fully automatic which has precluded their use in routine applications. Such a drawback follows the adoption of mathematical expressions relating particular field components of gravity and magnetic fields which necessarily requires a known magnetization direction in interpreting real data sets.

This article presents analytical expressions relating vectors of gravity and magnetic fields that enable one pass estimates for both magnetization-to-the-density-ratio (MDR) and magnetization inclination (MI). No inverse problem formulation, as done by Bott and Ingles (1972), is required, thus saving computer efforts. Tests with synthetic data sets illustrate the utility of the proposed technique to the joint interpretation of gravity and magnetic data.

**Basic equations**

By assuming 1) the sources generating the gravity and magnetic potentials are common; 2) the source magnetization direction is constant, and; 3) the MDR is constant, the Poisson theorem states (Grant and West, 1965; Blakely, 1995)

$$V = -p\frac{\partial U}{\partial m}, \quad (1)$$

where, V is the magnetic potential, U is the gravity potential, $\partial/\partial m$ is the directional derivative operator, **m** is a constant unit vector along the magnetization, and p is the Poisson ratio given by

$$p = \frac{\Delta M}{G\Delta\rho} \quad . \quad (2)$$

In equation (2), G is the gravitational constant; $\Delta\rho$ is the source density contrast, and $\Delta M$ its total magnetization (induced plus remanent) contrast. For sources such that, $\Delta\mathbf{M} = \Delta M\mathbf{m}$ (bold letters denoting vector quantities). The MDR is such that $r \equiv \Delta M/\Delta\rho$. For sources satisfying the Poisson conditions, the magnetic potential V can be obtained by deriving the gravity potential U or, conversely, the gravity potential U by integrating the magnetic potential V (Baranov, 1957). Corresponding expressions for the related vector fields are obtained by applying the 2D gradient operator, $\nabla \equiv \partial/\partial x\,\mathbf{e}_x + \partial/\partial z\,\mathbf{e}_z$, on both sides of equation (1). The anomalous vector magnetic field, $\mathbf{T}_m$, arising from sources with direction of magnetization, **m**, is thus obtained as

$$\mathbf{T}_m = -p\nabla\left(\frac{\partial U}{\partial m}\right). \quad (3)$$

Similarly, the magnetic field, $\mathbf{T}_z$, caused by the same sources but assuming vertical magnetization (i.e.: $\Delta\mathbf{M} = \Delta M\mathbf{z}$ ) is

$$\mathbf{T}_z = -p\nabla g_z, \quad (4)$$

where

$$g_z = \frac{\partial U}{\partial z}, \quad (5)$$

is the expression for the gravity anomaly; subscript z denoting the vertical component of the related gravity field, which commonly is measured in gravity exploration. However, it can be shown that for 2D homogeneous sources

$$|\mathbf{T}_m| = |\mathbf{T}_z| \quad , \quad (6)$$

for any magnetization direction $\mathbf{m}$. Since the symbol $|.|$ represents the Euclidean norm, equation (6) shows that the magnetic field magnitude (2D sources) is invariant with the magnetization direction. The information on the magnetization inclination solely resides in the inclination of the related vector magnetic field. Such properties of 2D magnetic fields is illustrated in Figure 1.

For sources satisfying the Poisson conditions, equation (4) can be substituted in equation (6) to give

$$|T_m| = |p\nabla g_z| . \quad (7)$$

from which the MDR absolute value, |r| , can be estimated:

$$r = G\frac{|\mathbf{T}_m|}{|\nabla g_z|}. \qquad (8)$$

Also can be verified that the angle between the vectors $\mathbf{T}_m$ and $\nabla g_z$ depends on the apparent magnetization inclination, $\alpha$ (or MI), which then can be determined by

$$\alpha = \operatorname{asin}\left(\frac{\mathbf{T}_m.\nabla g_z}{|\mathbf{T}_m||\nabla g_z|}\right) . \qquad (9)$$

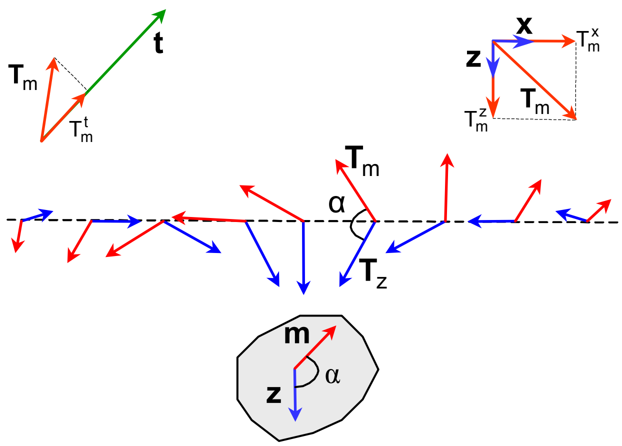


Figure 1- Schematic representation of the vector fields in equations (4) to (9): $\mathbf{T}_m$ (red) is the vector magnetic field from a source with magnetization along the unit vector **m**; $\mathbf{T}_z$ (blue) is the magnetic field from the same source except by considering a vertical magnetization, **z**. As equation (8) states, the magnitudes of the fields $\mathbf{T}_m$ and $\mathbf{T}_z$, are identical, whatever direction **m** and position along a profile. From equations (4) and (9), the angle • of the magnetization is equal to the angle between $\mathbf{T}_m$ and $\mathbf{T}_z$, at any station of a profile. For a inducing field (green) along unit vector **t**, the usually measured total field anomaly is the component $T_m^t$.

**Utility of solutions (8) and (9)**

Equations (8) and (9) are the basis of the proposed technique since they determine the parameters |r| and $\alpha$ at each station of a profile. Since the MDR and MI are determined, the proposed method will hereafter be referred as MDR-MI method. The model in Figure 2 helps us to assess the utility of the MDR-MI method in characterizing a multiple source region whose related anomalies, due to the effect of superposition, appear to be very complex (2c). Despite the anomaly complexity, true MDR and MI values are determined from equations (8) and (9) (Figure 2a). As illustrated in Figure 2b, the intensities $|T_m|$ and $|\nabla g_z|$ are perfectly correlated when the Poisson conditions are satisfied. This characteristic can be used to identify a region satisfying such conditions.

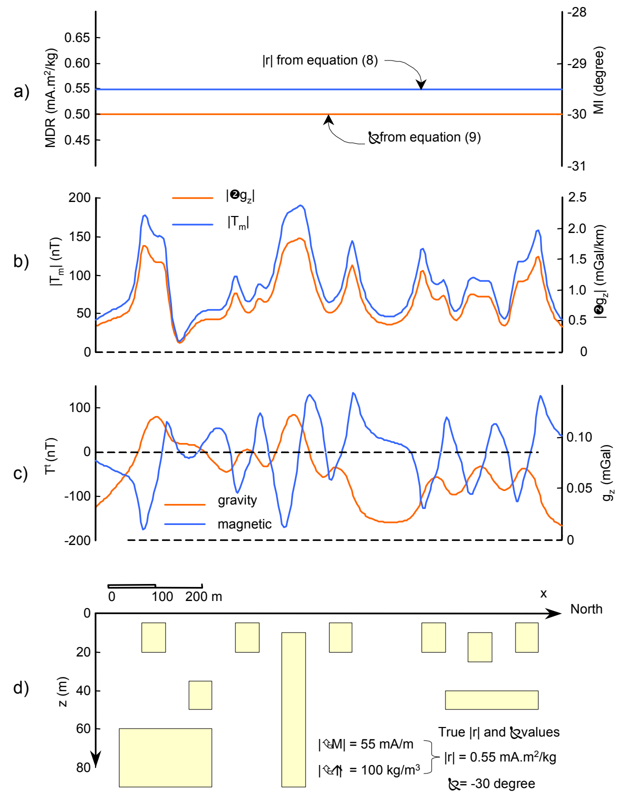


Figure 2 - MDR-MI profiles over a multisource prism model obeying the Poisson's conditions; a) MDR (blue) and MI (red) values; b) magnitudes of the vector magnetic field (blue) and gradient of the gravity anomaly (red); c) magnetic (blue) and gravity (red) anomalies; d) cross-section of the 2D prisms and physical property values.

**Data processing scheme**

To be evaluated from equations (10) and (11), the MDR and MI parameters require the knowledge of the vector fields $\nabla g_z$ and $\mathbf{T}_m$, which, in turn, require the gravity anomaly derivatives $\partial g_z/\partial x$ and $\partial g_z/\partial x$ and magnetic field components $T_m^x$ and $T_m^x$. Unfortunately, routine gravity and magnetic surveys only measure single field components: the gravity vertical component, $g_z$, and the magnetic total field component, $T_m^t \equiv \mathbf{t}.\mathbf{T}_m$, or its gradient. Here, the unit vector **t** denotes the direction of the geomagnetic field. Since homogeneous 2D sources are considered, the magnetic field $\mathbf{T}_m$ has components only along the x and z axes. The projected vector, $\mathbf{t}_{xz}$, obtained by projecting vector **t** onto the x-z plane, is given by $\mathbf{t} = L\mathbf{e}_x + N\mathbf{e}_z$ where $l' = \cos(\alpha)$, $N = \sin(\eta)$ and $\eta = a\tan[\tan(I_g)/\cos(D)]$ is the apparent inclination; $I_g$ is the geomagnetic field inclination, and D is such that $D \equiv D_g + S$. The angel $D_g \equiv D - S$ is the geomagnetic declination, and S the source strike, positive clockwise measured with respect to the North. Due to the intrinsic properties of the potential fields, the required components

$\partial g_z/\partial x$, $\partial g_z/\partial x$, $T_m^x$ and $T_m^x$ can be determined at any point away from the causative sources simply by applying a suitable set of linear transformations upon the measured anomalies. In the wavenumber domain, the linear transformations can be carried out according the flowchart presented in Figure 3.

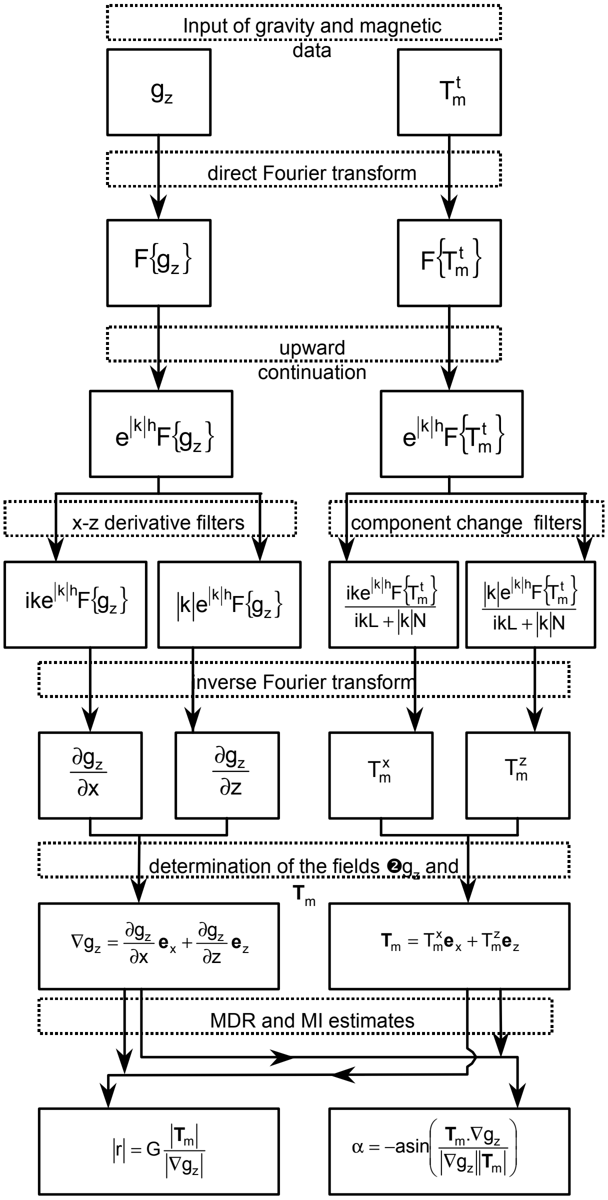


Figure 3- Data processing flowchart to determine the MDR and MI parameters. Definition of mathematical terms: h, continuation height (negative upward); F direct Fourier transform; k Fourier domain wavenumber. Dotted line boxes assign instructions and solid line ones the results from such instructions. Further information about the upward continuation and component change filters can be found in Gunn (1975) and Blakely (1995).

As indicated in Figure 3, the processing routine incorporates a step in which both gravity and magnetic data are upward continued. This operation was included in order to prevent excessive noise amplification in computing the gravity gradient.

**Synthetic tests**

To gain insight to the expected MDR-MI performance in more complex environments, three cases of synthetic MDR-MI responses are presented (Figure 4). These responses were evaluated from a geophysical models consisting of two sets of sources, each side using several 2D prisms (Figure 4e).

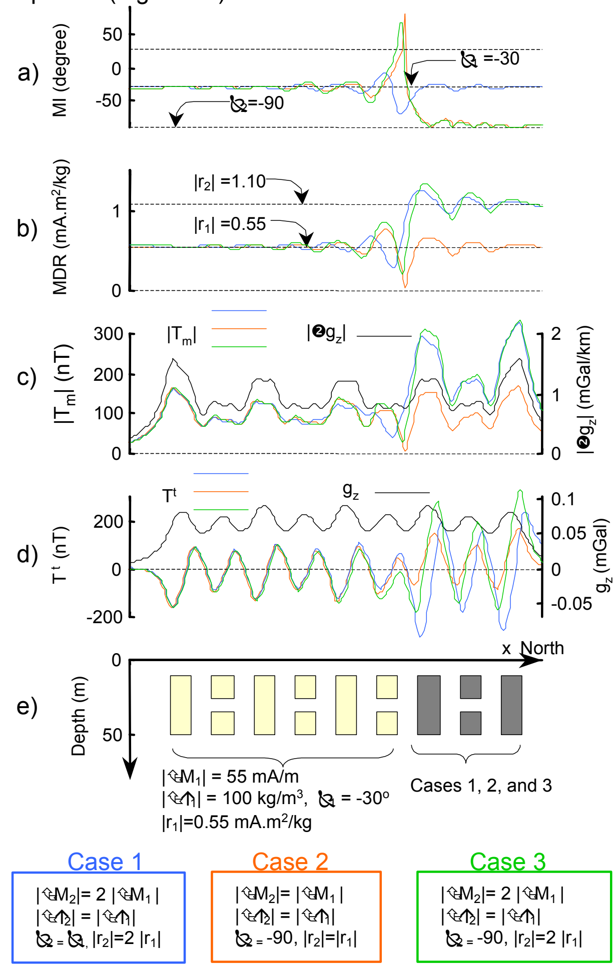


Figure 4 - MDR-MI profiles above multisource media representing different types of transition zones (cases 1 to 3); a) MI - Magnetization Inclination; b) MDR - Magnetization-to-density-ratio; c) vector field magnitudes $|T_m|$ (colored according each case) and $|\nabla g_z|$ (black); d) gravity (black) and magnetic (colored) anomalies; e) prismatic bodies and properties.

As Figure 4 shows, at stations far from the transition zone the MDR and MI parameters are correctly determined in all of the tested cases. The rather flat trends over the homogeneous blocks allow the identification of the regions satisfying the Poisson conditions. Spurious MDR-MI values only occur close to the transition of source types because in this region the gravity and magnetic fields are mostly affected by the two set of differing sources. Close to the transition, MDR-MI estimates are only apparent and, as such, may present no direct correspondence with the true properties of the underlying sources. Apparent MDR-MI estimates can reach values outside the range of the two sets. Nevertheless, the oscillation of the apparent values near the transition zone denotes its presence which in some cases is not very evident in the gravity and magnetic profiles (Figure 4d). It suggests a further application for the proposed method. Besides a physical property profiler, the MDR-MI method mighty, in some cases, detect the variation between (or within) geological units with MDR or MI contrast. Another feature observed in Figures 4c and 4d is the rather uncoupled variations exhibited by the MI and MDR profiles. In case 1, for example, the MDR apparent values adequately identify the existing variation while the MI values only oscillate around the true inclination value. The MI estimates are not severely distorted by the MDR variation thus establishing the uncoupled characteristic previously described. Uncoupled response is also noted in case 2. In case 3, it allows us to map the joint variation of MDR and MI properties as when isolated variations were considered (cases 1 and 2). In favorable conditions, this MDR-MI uncoupled response could be used to identify which Poisson condition is (are) violated. Tests not presented here suggest the ability to identify gradational variations in the MDR and MI rock properties, a feature practically invisible in the corresponding anomalies.

**Conclusions**

The MDR-MI method can easily be implemented to existing software packages and its results promptly can be interpreted. Regions where the Poisson conditions are satisfied are automatically identified from a well defined flat pattern in both MDR and MI profiles (mainly in the former one). Their boundaries can also be inferred since notable variation occurs close the contacts.

Further synthetic tests and results from the real data applications are presented by (Mendonça, 2003). In real data applications, two main limitations were observed. First, the proposed method requires very elongated anomalies thus requiring a proper profile positioning within the gravity and magnetic anomaly maps. Secondly, the profile must encompass sources with a same density contrast sign (note the Poisson's conditions are violated if density contrast changes), which implies either negative or positive gravity anomalies but not both them simultaneously.

**Acknowledgments**

This research was supported in part by the grants 301439/91-5 and GTM-01/97-02/01 from CNPq-Brazil.

**References**

Baranov, V., 1957, A new method for interpretation of aeromagnetic maps: pseudo gravity anomalies: Geophysics, **22**, 359-382.

Blakely, R. J., 1995, Potential theory in gravity and magnetic applications. Cambridge University Press.

Bott, M. H. P. and Ingles, A., 1972, Matrix method for joint interpretation of two-dimensional gravity and magnetic anomalies with application to the Iceland-Faeroe Ridge: Geophys. J. Roy. Astr. Soc., **30**, 55-67.

Chandler, V. W., Koski, J. S., Hinze, W. J., and Braille, L. W. , 1981, Analysis of multisource gravity and magnetic anomaly data sets by moving-window application of Poisson theorem: Geophysics, **46**, 30 19.

Chandler, V.W. and Malek, K. C.,1991, Moving-window Poisson analysis of gravity and magnetic data from the Penokean Orogen,east-central Minnesota: Geophysics, **56**, 123-132.

Cordell, L. and Taylor, P. T., 1971, Investigation of magnetization and density of a North American seamount using Poisson's theorem: Geophysics: **36**, 919-937.

Grant, F. S. and West, G. F, 1965, Interpretation theory in applied geophysics. McGraw-Hill.

Garland, G. D., 1951, Combined analysis of gravity and magnetic anomalies: Geophysics, **16**, 51-62.1

Gunn, P. J., 1975, Linear transformations of gravity and magnetic-fields: Geophys. Prosp., **23**, 300-312.

Hildebrand, T. G., 1985, Magnetic terranes in the central United States determined from the interpretation of digital data, in Hinze, W. J. Ed., The utility of gravity and anomaly maps: Soc. of Expl. Geophys., 248-266.

Kanasewich, E. R. and Argawal, R. G., 1970, Analysis of combined gravity and magnetic fields in wave number domain: J. Geophys. Res., **75**, 5702-5712.

Mendonca, C. A, 2003, Automatic determination of the magnetization-to-density ratio and the magnetization inclination from the joint interpretation of 2D gravity and magnetic anomalies: Geophysics (in press).

Ross, H. P. and Lavin, P. M., 1966, In situ determination of the remnant magnetic vector of two-dimensional tabular bodies: Geophysics, **31**, 949-962.